TECHNICAL NOTES

"Technical Notes" in the Journal of Rehabilitation Research and Development most often originate when an investigator, in the course of his research, pauses to record the details of a device and/or procedure which has contributed materially to furthering the scientific purposes of his research. We publish them in the hope that they will become *part of the universal exchange of scientific instrumentation and device "shop talk."*

"Technical Notes" found in the Journal will usually lack controlled comparison studies vis-a-vis alternate ways of accomplishing similar ends; they are clearly not complete reports of scientific research. Nevertheless, they are thoughtfully reviewed by members of our editorial board and by such ad hoc reviewers as may seem appropriate, in order to assure you of their originality, technical correctness, medical appropriateness, etc.

Measurement of Weightbearing[a] During Standing

J. J. POYEZDALA, B.S.

R. J. JAEGER, Ph. D.*

Pritzker Institute of Medical Engineering
Illinois Institute of Technology

Introduction

During stance with balance aids, it is often difficult to judge the amount of weight actually being borne by the lower versus the upper limb. This probably explains much of the continuing interest, in the field of rehabilitation medicine, in the problem of measurement of the weight borne by the legs during standing.

The purpose of this study was to construct a device to continuously monitor the weight borne by the lower extremities of disabled individuals during standing. It was desired that the device have general clinical utility. Accurate measurement of total weight, weight borne by each leg, and the difference in weight distribution between the two legs was required. It was desired that the output be capable of direct connection either to a chart recorder or to an analog-to-digital converter for computer processing. Furthermore, it was deemed essential that the device be simple to use, without complicated transducer attachments or calibration procedures.

A variety of devices have been proposed to make these measurements. One which has received extensive clinical evaluation is the "Limb Load Monitor" (1). Other devices have been reported that measure the load at the heel and metatarsals (2), at 6 locations along the foot (3), at 16 points on each foot (4), and at 8 points on each foot (5). These devices are all capable of being used during gait, but it is sometimes difficult to calibrate the devices and make all the appropriate transducer attachments.

Single measurements of pressure distribution have been made with pressure-sensitive film (6) or dynamically with a device called the "footprint" (7). In some cases clinicians have used regular bathroom scales (8), which have the advantage of simplicity but the disadvantage of poor display of weight borne. Fully instrumented biomechanics platforms are also available (9); these measure all components of the ground reaction vector. One disadvantage of such platforms is cost.

Because none of the aforementioned devices meet the design criteria sufficiently well to warrant adoption for this study, a new device was constructed.

Methods

The device was to be designed for use only during quiet standing. Design considerations were further constrained by the desire to use commercially available equipment and minimize the amount and complexity of custom-built circuitry. This was done to make it as simple as possible for others to construct such a device.

A pair of digital scales (Heath-Kit Model GD-1186) were selected for transduction and numerical display of vertical force. The scales' commercial electronics were modified to accomodate AC line power instead of their original battery complement of six "D" cells each. Conversion was simply accomplished by removing the now unnecessary +5-volt regulator and low-battery-indicator driver transistors, replacing a filter capacitor rated at 10 WVDC with one rated at 25 WVDC, and connecting regulated +5-volt and +12-volt supplies to the circuit boards.

The additional circuitry performs scaling, filtering, and analog computation of the weight borne by each leg (R and L), total weight (R + L), and the difference in weight between left and right legs (R - L). Schematic diagrams of the custom electronics are shown in Figure 1. The instrumentation amplifier (Fig. 1A) is connected directly to the strain gage bridge in the corresponding scale and is used to minimize noise and drift. Overall zero of the scale amplifier is set by input-nulling the instrumentation amplifier. A variable-gain amplifier follows that accomplishes calibration of overall circuit gain, and incorporates a 20 DB/decade low-pass filter with a cutoff frequency of 10 Hz. The sum amplifiers (1B) and difference amplifiers (1C) are standard design.

The modified scale electronics, the custom circuitry, and a commercially manufactured triple output (+5, +12, and −12 volts) power supply (Power-One model HTAA-16W-A) were packaged together in a metal enclosure 5 in high, 12 in wide and 3.5 in deep. Figure 2 shows the completed enclosure mounted on the platform.

In addition to the digital display of the weight borne by each leg, located in the enclosure mounted on the platform, provision was made to add one or more auxiliary displays that could also be readily viewed by the subject to provide visual feedback of dif-

[a]This work was supported in part by the Paralyzed Veterans of America.

*Address correspondence to R. J. Jaeger, Ph. D., Pritzker Institute of Technology, Chicago, Illinois 60616. Tel. (312) 567-5324.

ferent aspects of weightbearing. One such display incorporates a horizontal row of four 10-segment LED bar/dot displays (Fig. 3 and 4). These displays are driven in dot mode to indicate in a semi-quantitative manner the difference in weight between left and right legs. When the two legs each bear the same weight, the center dot in the display is lit; if the left or right leg bears more weight, the dot moves left or right, respectively, with each succeeding dot indicating an additional weight differential of 5 kilograms. A second added display provides two vertically-oriented LED displays, each showing the weight on the respective leg.

In order to provide for the greatest flexibility in both present and future auxiliary display designs, only the left (L) and right (R) weight signals are sent to the auxiliary display, and any desired further processing is done at that point. Thus, it was necessary to include a difference amplifier in the display. The chain of zener diodes shown is necessary to provide a linear display quantization of 5 kg/dot.

A square platform having overall dimensions of 36 inches on a side and 2¼ inches in depth was constructed of high-density particle board. In order to recess the scales to make their tops flush with the surface of the platform, three sheets of 3/4-inch particleboard stock were laminated together. The top two sheets were cut out to accomodate the scales prior to lamination, and filler blocks were retained to allow positioning of the scales in two different ways. Finally, the platform was covered with black plastic laminate for appearance and durability. A frame of $1^5/_8$-inch aluminum pipe was added to aid the disabled subject in standing

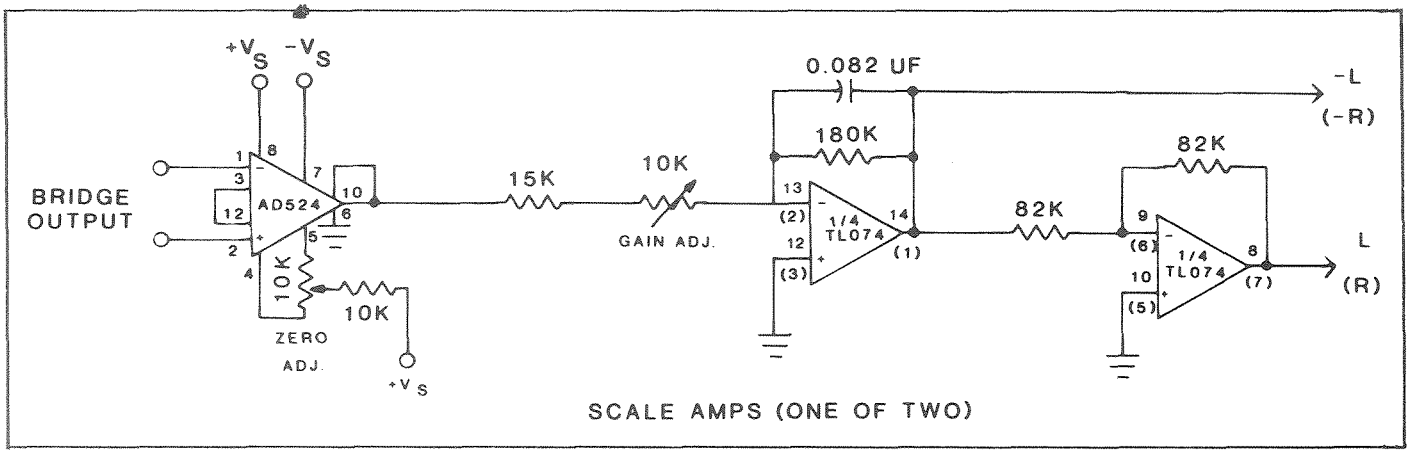

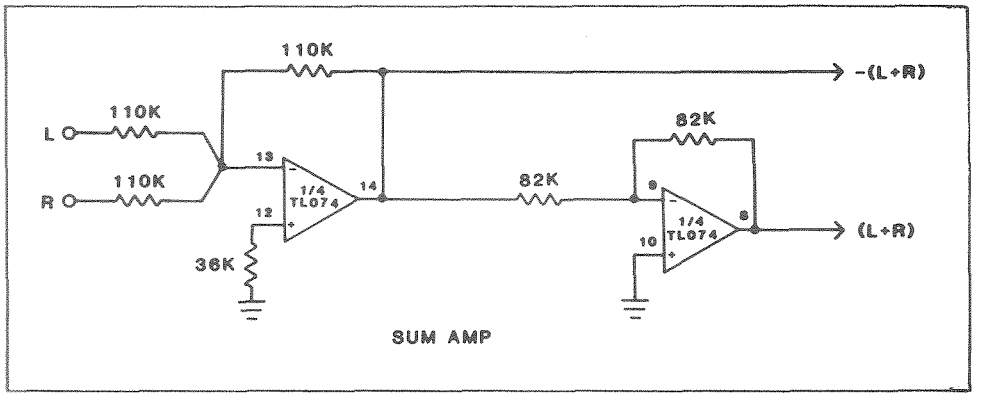

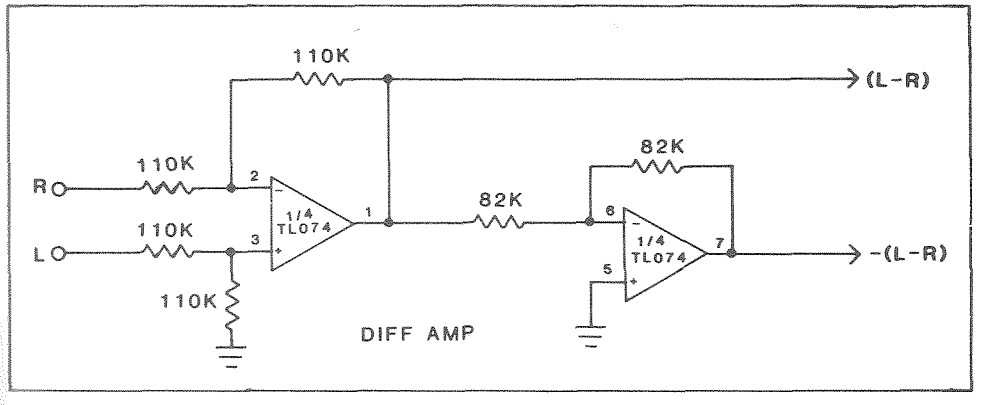

FIGURE 1
Schematic of custom-built electronics to interface existing commercial circuitry. A: Instrumentation amplifier, gain stage, and filter. B: Summing amplifier. C: Difference amplifier.

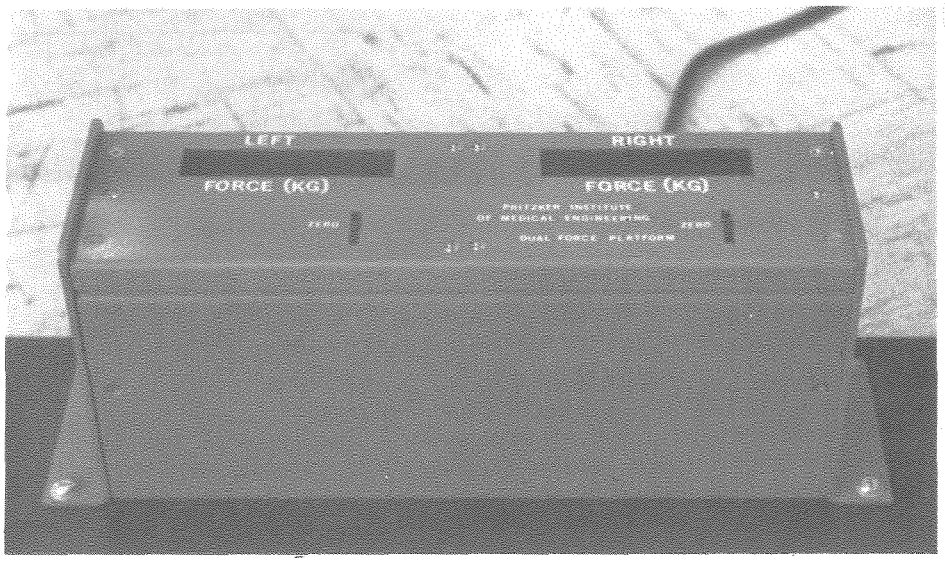

FIGURE 2
Close-up of electronics enclosure mounted on platform. The separate three-digit LED displays of weight on each scale are used for calibration. Zero potentiometers are also visible.

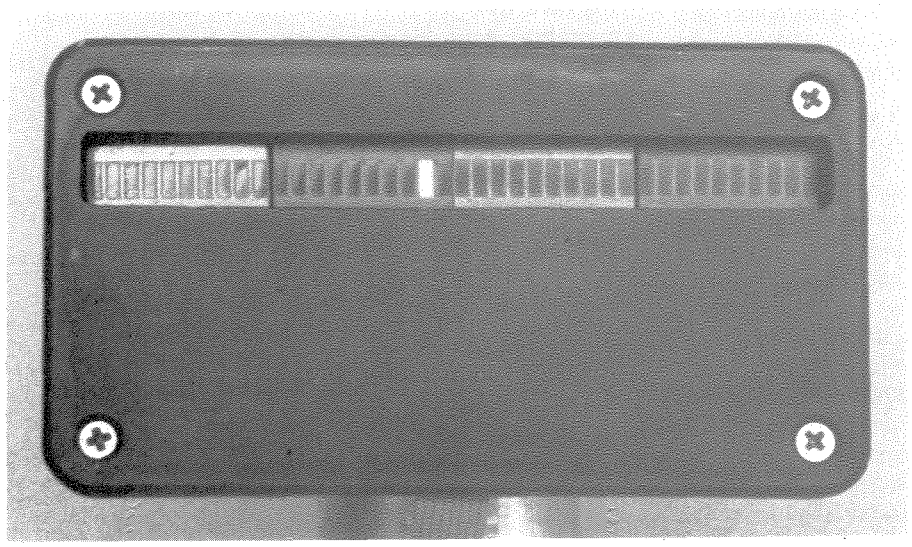

FIGURE 3
Close-up of one of the LED displays. In this case, a center LED is on if the weight is evenly distributed between the legs. The dot shifts either right or left as weight is transferred.

FIGURE 4
Schematic of LED display. The same basic configuration of LM3914's is used in other displays.

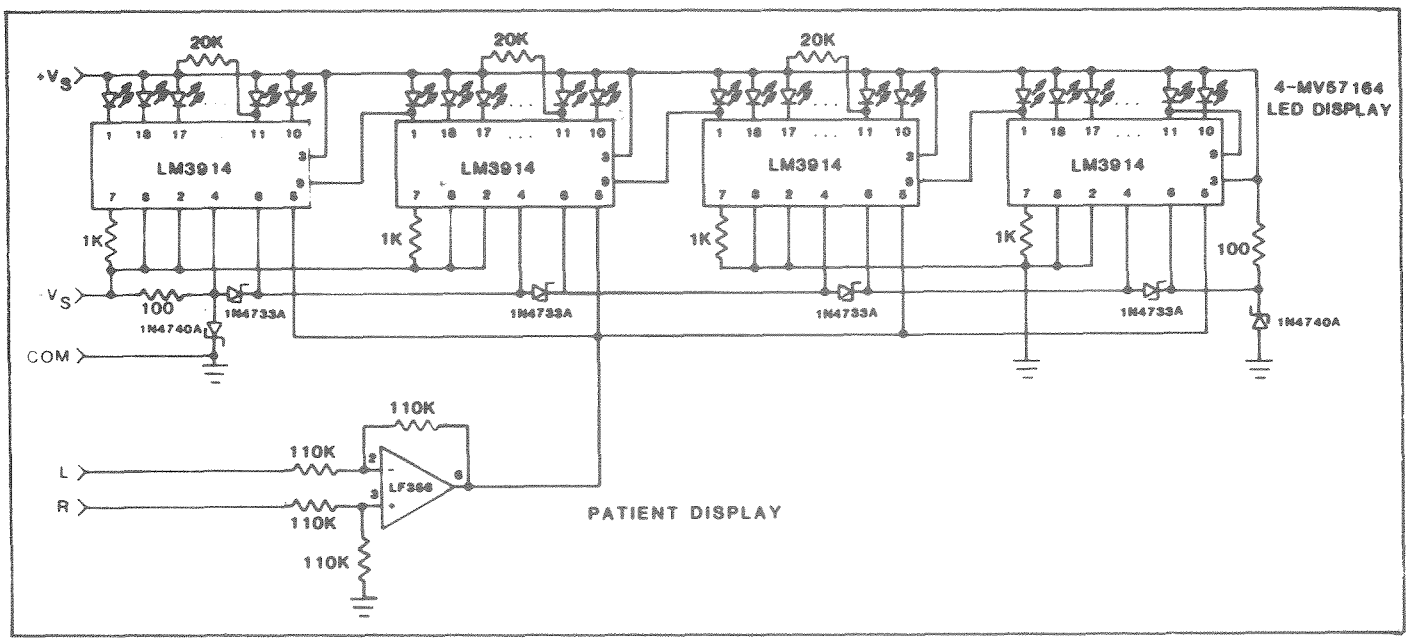

and balance. Mounted on the platform is the enclosure containing the electronics, and attached to the pipe frame is the patient display (Fig. 5).

Results

Calibration of the custom electronics consists of adjusting the output of each scale amplifier to zero with no weight on the scale, and then adjusting the gain appropriately with known weights on the scale. This procedure yields a linear static calibration curve with a standard output of 0.1 v/kg. Noise is about 3 millivolts RMS and drift is less than 0.001 v/hr after a 10-minute warmup period to allow the strain gages to stabilize. Calibration has been checked with each use—but recalibration has never been required.

Calibration of the commercial electronics is done in a similar manner, following the manufacturer's instructions.

In more than a year of operation, neither mechanical nor electronic failure has been experienced. The device is presently used with a two-channel stripchart recorder (Gould-Brush Model 220) and a PDP 11/45 computer with A/D converters.

A number of experiments have been performed on both normal and paraplegic individuals to study weightbearing and weight shifting. Paraplegic individuals stood by means of conventional knee-ankle-foot orthoses and bilateral electrical stimulation of the quadriceps muscles (10). Typical data for a normal and a paraplegic individual are shown in Figure 6 ■

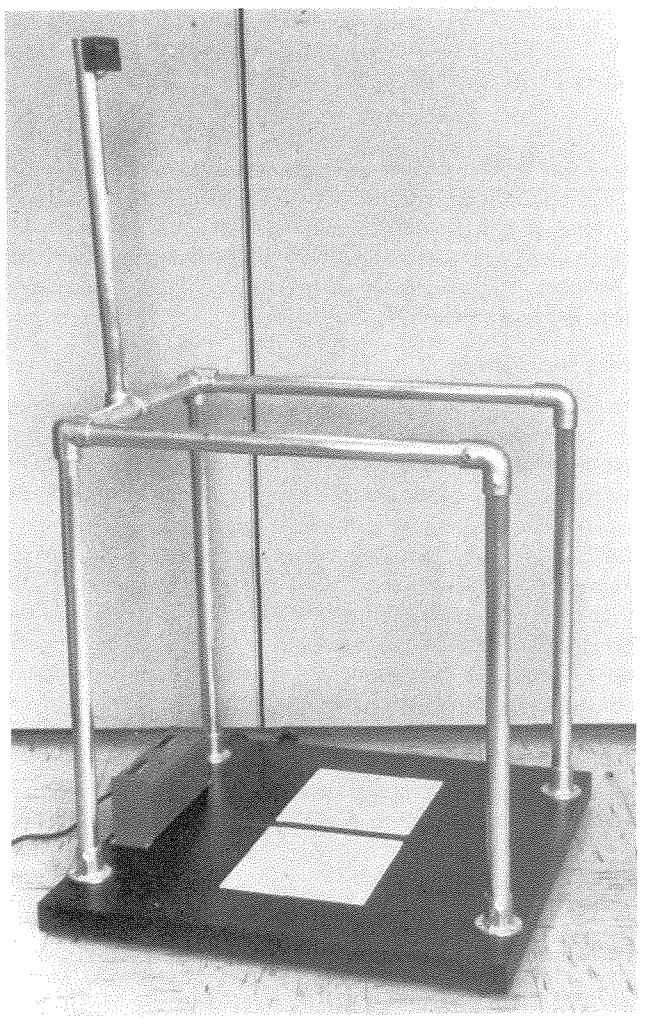

FIGURE 5
The dual vertical force platform. Each scale can be seen to the right and left of the center of the platform. The electronics package (Fig. 2) is mounted on the platform (left side in photo). The small enclosure at the very top houses the LED display (Fig. 3).

Turn page for Figure 6.

REFERENCES

1. Wannstedt G and Craik R: Evaluation of the Limb-Load Monitor. Technical Report TR1-78, Moss Rehabilitation Hospital, Philadelphia PA, 1977.
2. Miyazak S and Iwokura H: Limb-load alarm device for partial-weight-bearing walking exercise. Med & Biol Engng & Comput 16:500-506, 1978.
3. Tibarewala D and Ganguli S: Biomechanical evaluation of human lower-extremity disability in erect standing. Med & Biol Engng & Comput 21:91-96, 1983.
4. Soames RW, Stott JRR, Goodbody A, Blake CD, and Brewerton DA: Measurement of pressure under the foot. Med & Biol Engng & Comput 20:489-495, 1982.
5. Klajic M, Krajnik J, and Trnkoczy A: Determination of ground reaction and its distribution on the foot by the measuring shoes. XII Intl Conf Med & Biol Engng, Jerusalem, 40.1, 1979.
6. Aritomi H, Moritz M, and Yonemoto K: A simple method of measuring the footsole pressure of normal subjects using prescale pressure-detecting sheets. J. Biomech 16:157-165, 1983.
7. Simkin A and Stokes IAF: Characterization of the dynamic vertical force distribution under the foot. Med & Biol Engng & Comput 20:12-18, 1982.
8. Warren CG and Lehmann JF: Training procedures and biofeedback methods to achieve controlled partial weight bearing: an assessment. Arch Phys Med Rehab 56:449-455, 1975.
9. Hufschmidt A, Dichgans J, Mauritz KH and Hufschmidt M: Some methods and parameters of body-sway quantification and their neurological applications. Arch Psychiat Nervenkr 228:135-150, 1980.
10. Bajd T, Kralj A and Turk R: Standing-up of a healthy subject and a paraplegic patient. J Biomech 15:1-10, 1982

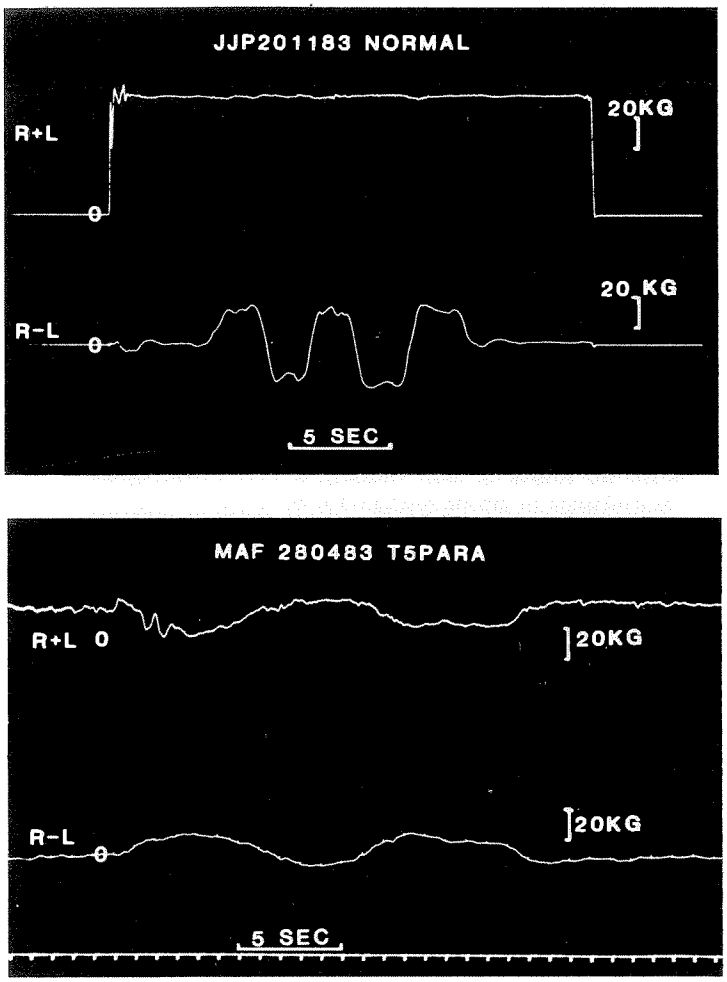

FIGURE 6
Typical weight-shifting data for a normal individual (A) and a paraplegic individual (B). Total weight borne by the legs (R + L) and difference in weight distribution between legs (R − L) are shown. Both subjects were instructed to stand quietly and then shift weight from left to right. In the case of the normal subject a difference in weight born by the legs could easily be plus or minus 20 kg, with no shifting of body weight to the hands. The paraplegic subject could not perform comparable shifting without transferring some of his body weight to the balance frame via the upper extremities.

Qualitative and Quantitative Gait Phase Analysis by Continuous Monitoring of Inter-Ankle Distance

MICHAEL S. PINZUR, M.D.[a]
PHYLLIS DIMONTE LEVINE, R.P.T.
JOHN TRIMBLE, Ph.D.
KENNETH HAAG, Ph.D.
RICHARD SHERMAN, M.D.

Rehabilitative Research and Development Center
Hines Veterans Administration Hospital
Hines, Illinois 60141

Department of Orthopaedics and Rehabilitation
Loyola University Medical Center
Maywood, Illinois 60153

Abstract—A new device is presented that is able to provide a temporal recording of gait as well as a continuous qualitative monitoring of gait events. It can be used with motor-point electromyography to perform walking electromyography, with an electrogoniometer to record joint position, or with other measuring devices to record events relative to phase of gait. The major advantages of this system as compared with available systems are (i) ease of use, (ii) decreased patient encumbrance, (iii) potential for portability, (iv) greatly reduced expense, and (v) the potential for digitizing the signal for computer compatibility. Preliminary data are comparable to available accepted norms.

Introduction

This paper reports on a simple new device which is able to provide a temporal recording of gait events including a qualitative monitoring of gait events. Developed in the VA Rehabilitation Research and Development Center at Hines Veterans Administration Hospital, it was originally utilized as a qualitative measure of mobility in blind patients (1, 2).

System description

The ultrasonic limb-position monitor is based on a measurement of the time required for a pulse of ultrasonic energy to propagate from a transmitter transducer on one ankle to a receiver transducer on the other ankle. The propagation path for the ultrasonic energy is shown schematically in Figure 1.

During operation, the transmitter transducers are simultaneously energized with short pulses of electrical energy. This electrical energy is converted to a sinusoidal burst of acoustical energy by the ultrasonic transducers. The frequency of the sinusoid is equal to the resonant frequency of the transducer, which is chosen to be above the normal audible range to avoid disturbing the user and to diminish interference from ambient acoustic energy.

The acoustic energy propagates away from the transmitters at the velocity of sound. When the wave front is intercepted by a receiver transducer, it is converted to electrical energy by the transducer. The time required for the acoustic energy to pro-

[a]Please address all correspondence to: Michael S. Pinzur, M.D., Department of Orthopaedics and Rehabilitation, Loyola University Medical Center, 2160 South First Avenue, Maywood, Illinois 60153.

pagate from the transmitter transducer to the receiver transducer is a measure of the geometric distance between the transducers.

The physical relationship between distance, time, and velocity is $d = v_s t$ where d is the distance between transducers, v_s is the velocity of sound, and t is the time required for the acoustic energy to propagate between transducers. Since the speed of sound in air is a constant for any specific temperature, pressure, and humidity, a measure of the propagation time is linearly proportional to the distance traveled.

The basic functions required to generate and process the electrical signals associated with the transducers are shown in Figure 2. A pulse generator sends pulses of electrical energy to the transmitter transducers at a predetermined repetition rate. In the present implementation of the device, this rate was chosen to be approximately 100 pulses-per-second. For a normal stride rate of up to two strides-per-second, this pulse repetition rate gives 50 or more measurements of instantaneous interankle separation during each stride.

Both of the receiver transducers may intercept the transmitted acoustic energy and generate an electrical signal. However, except for midstride position, there always exists one combination of transmitter and receiver transducers for which the distance between them is least. This least distance corresponds to the shortest time between transmitter excitation and receiver response. Therefore, the propagation time measurement is initiated when the transmitters are excited and is teminated when the first electrical sign is generated by either of the receiver transducers. At midstride, both receiver transducers intercept acoustic energy simultaneously and, therefore generate an electrical signal at the same time.

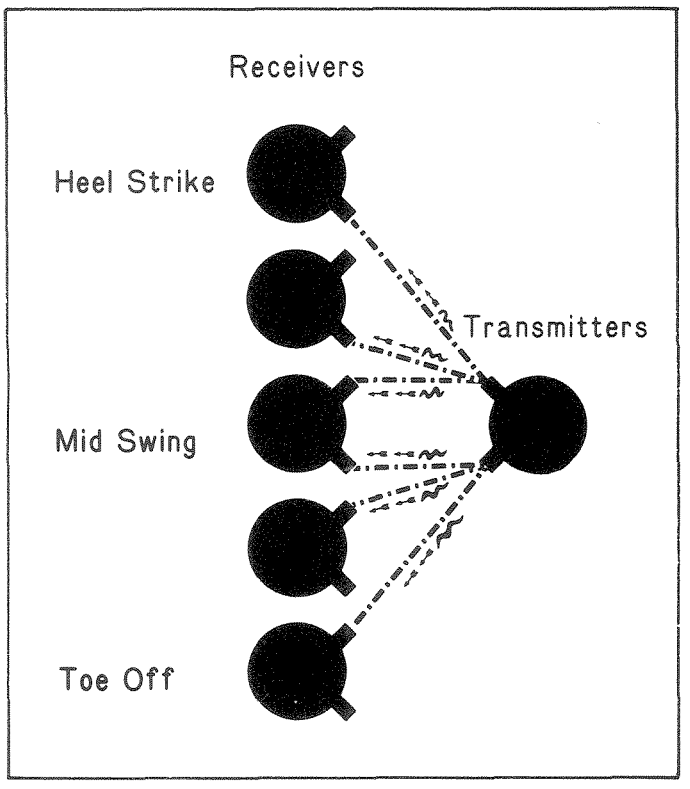

FIGURE 1
Propagation path for relative positions of ankles during stride.

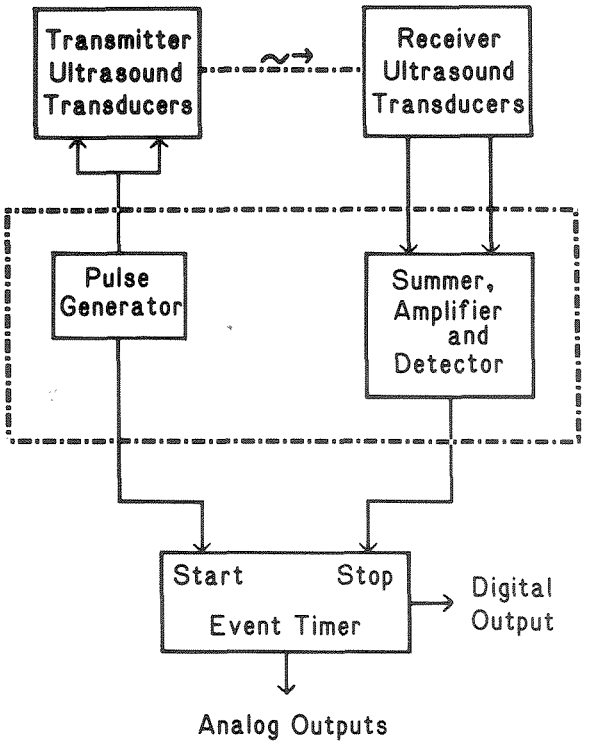

FIGURE 2
System functional diagram.

The event timer measures the time that elapses between the application of an electrical signal to the Start input and an application of an electrical signal to the Stop input. Each measure of time is converted to an analog voltage proportional to the elapsed time and to the derivative of elapsed time. A digital signal with binary value proportional to elapsed time is also produced.

The analog voltages can be displayed on an oscilloscope or recorded on a strip chart recorder to obtain a real-time record of the gait characteristics. The digital output signal can be recorded on magnetic tape or other medium for future computer analysis to obtain velocity, acceleration, and other stride features of interest.

The pulse generator and the summer-amplifier-detector circuits are mounted in a small box (2 × 3 × 5 inches) which is attached by a waist belt to the person being studied. The event timer is located at a stationary site and receives electrical signals by means of thin, flexible 30-foot cables attached to the waist-mounted box (Fig. 3-A).

Methods

The device is a simple ultrasonic transmitter and receiver system which, with associated electronics, provides a continuous recording of the distance between transmitter and receiver and thus delivers a continuous monitoring of the "inter-ankle distance" (IAD). Two transmitter transducers and two receiver transducers are snugly attached with Velcro straps just above the medial malleoli. As shown in Figure 3-B, one of the transducers is directed 60 degrees forward and the other 60 degrees rearward. This provides nearly equal signal reception over the entire range of the stride.

A sample tracing is shown in Figure 4. The uppermost point on the tracing represents the period of double-support and the

FIGURE 3A
Patient undergoing a walking EMG.

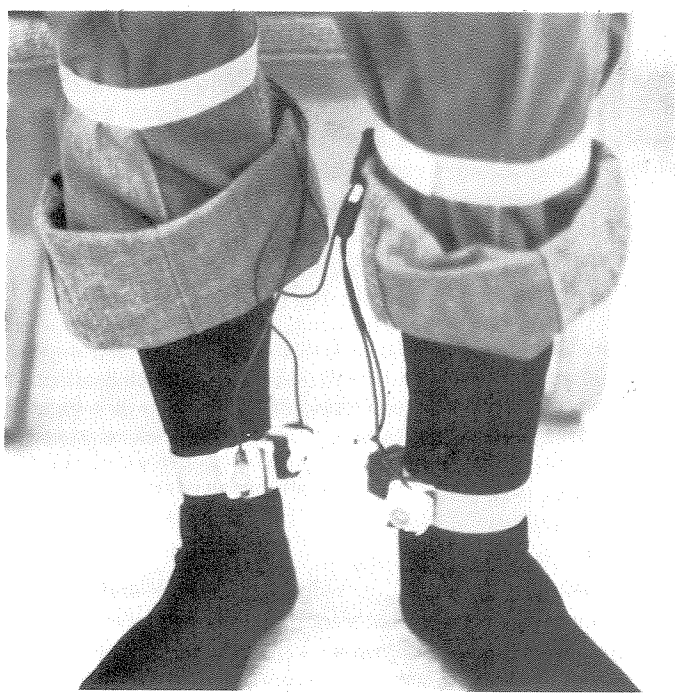

FIGURE 3B
This device marks use of an ultrasonic transmitter strapped to one ankle and receiver to the other.

lowermost point represents mid-swing. There are two periods of constant interankle velocity (constant slope of IAD tracing) between toe-off and midswing and between midswing and initial contact. Initial contact (heel-strike) occurs at the time of change in slope of the IAD upward tracing. Toe-off occurs at the downstroke change in slope. For simplicity, the recording is marked at right heel-strike to label right and left steps. Once these events are identified, the stance, swing and double-support times are easily obtained. The signal that produces this recording can be digitized and calculations performed by a microprocessor.

Results

Forty volunteers between the ages of 24 and 43 were used in the present study. There were 20 men and 20 women with average ages of 31 (male) and 33 (female). None of the subjects displayed any gait abnormalities by observational analysis. The transmitter transducers were snugly attached to the right leg just above the flare of the medial malleolus and the receiver transducers were similarly attached to the left leg. Each subject was asked to walk at his/her self-selected velocity along a 25-foot flat linoleum walkway. Four such recordings were performed on each subject. Stance, swing, and double-support times were determined by the average values obtained from the four recordings.

The average cadence was 102.04 steps per minute with forward velocity of 80.12 centimeters per second. Paper speed was 25 millimeters per second. By determining the absolute amount of time spent in each phase of gait (Fig. 5), relative percentages of the gait cycle were calculated. Stance phase occupied an average of 61.49 percent of the gait cycle, swing phase 38.51 percent and double support 13.04 percent.

Discussion

The object of this study was to validate a new device and suggest its value in temporal recording of gait events. The device also provides a continuous qualitative monitoring of gait which can be related to specified events. The analyzer is compact and easy to utilize with a minimal amount of technical expertise and training. A walking elctromyogram can easily be performed by one in-

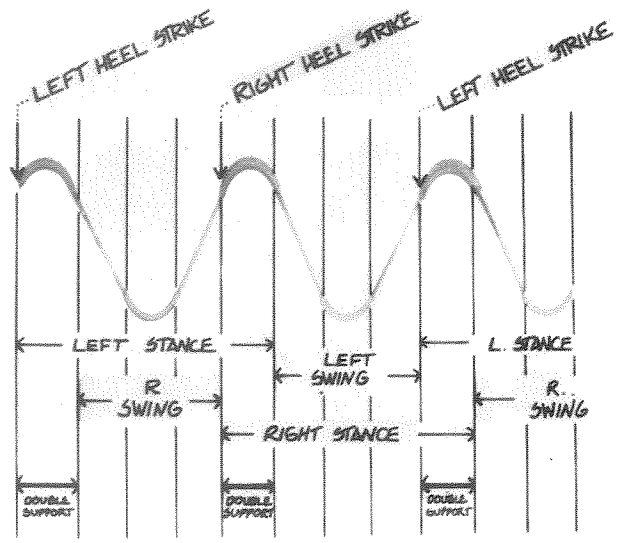

FIGURE 4
Sample IAD curve showing temporal phases of gait.

dividual in less than 40 minutes. The system is extremely light in weight and non-encumbering, with each transducer weighing less than 100 grams and the entire attached device weighing well under 1 kilogram. Portability is available, as the entire attached electronics including strip-chart recorder can be placed on a 0.5 × 1.5 meter portable cart. Due to the nature of the signal, it can easily be digitized for input into a computer system. The quantitative data compares very favorably with the accepted norms presently available (3). In addition, the entire device can be inexpensively fabricated for less than $1500.

Summary

A new device is presented that can be utilized as a temporal recorder of gait. Its value is in its (i) ease of use, (ii) decreased patient encumbrance, (iii) portablity, (iv) reduced expense, (v) computer compatablity, and (vi) accuracy ■

REFERENCES

1. Murray MP: Gait as a total pattern of movement. Amer J Phys Med 46:290, 1976.
2. Trimble JL and Hollyfield RL: An inexpensive ultrasonic device for measuring the walking pattern of blind people. (Submitted)
3. Hollyfield RL and Trimble JL: Measuring Performance by Blind Travelers. Paper presented at the Fourth Annual Conference on Rehabilitation Engineering, August 20-September 3, 1981.

FIGURE 5
IAD as a temporal marker for performing a walking EMG in a normal subject. The block marks stance phase. The lower channel is the electrical activity recorded from a surface electrode mounted at the motor point of the tibialis anterior. The middle channel records a filtered EMG signal which can be digitized for computer compatability.

Inkbraille as a Potential New Reading System for the Blind[a]

DAVID W. HISLOP, B.S.*,
B. L. ZUBER, Ph. D*+
JOHN L. TRIMBLE, Ph. D.+

+Rehabilitation Research and Development Center
Hines Veterans Administration Hospital
Hines, Illinois 60141

*Department of Bioengineering
University of Illinois at Chicago
Chicago, Illinois 60680

Abstract—Inkbraille, a reduced size ink-image version of the familiar braille code, was conceived in an attempt to sidestep the major disadvantages of embossed braille, while retaining the unsurpassed reading rates achieved by the blind using that code.

Inkbraille would ultimately be translated by a specially designed hand-held electronic device with appropriate tactile output. Such a device is not yet available, so In this study we test the readability of Inkbraille when read by means of a commercially available electronic reading aid, the Optacon, which presents its output tactually on a field of vibrating pins which are sensed with a finger. Three modes of tactual reading were compared: (i) conventional embossed braille, and (ii) the Opticon's vibrating-pin-field presentation of typed letters and (iii) its presentation of Inkbraille.

All subjects were able to read Inkbraille upon initial exposure. Subjects who were tested in multiple sessions exhibited significant increases in Inkbraille reading rates after only limited exposure. Since Inkbraille and letterprint reading rates were the same in this study, the results led the authors to conclude that a rate limitation may have been imposed by the device (the Optacon) that was used to translate both the Inkbraille and the letterprint.

Introduction

Embossed braille reading rates of about 100 words-per-minute (WPM) are not unusual (Foulke, 1982 (1)). No other tactile-based reading system allows the blind to read at such a high rate. The braille code offers further advantages in that it is linguistically relatively efficient (Grade II braille) and it is in rather widespread use among the blind population. There are, however, major disadvantages to embossed braille. Reading materials in this medium are bulky, they are costly to produce, store, and distribute, and they are subject to deterioration through repeated use.

A reading aid that would convert an ink-image of the braille code to a direct tactile facsimile (Fig. 1) might retain the high reading-rate advantage of embossed braille while eliminating the major disadvantages of that medium. It was this thought that led to the conception of Inkbraille (Hislop, Zuber and Trimble, 1983a (2)) as a possible input code for a new "reading system."

Inkbraille can be simply and inexpensively produced on ordinary paper, using conventional printing techniques, and its use could result in books for the blind of a size similar to those for the sighted. The decreased bulk of Inkbraille, as compared to embossed braille, could result in significant economies related to storage and distribution, and could also enhance the possiblity of individual ownership of reading materials by the blind.

Inkbraille as currently configured is a reduced-size ink-image version of the familiar braille code. In this pilot study we address the concerns of Inkbraille production, test its readability, and investigate the ease with which skilled readers of embossed braille can learn to read a tactile output based on Inkbraille.

Methods

In the absence of a tactile-output device designed specifically to "read" Inkbraille, we decided to use the tactile Optacon (Bliss, 1970 (3)) as a means of testing Inkbraille. This was convenient in that there was an Optacon available to the authors, who were familiar with the characteristics of Optacon reading (Hislop, Zuber, and Trimble, 1982 (4), and 1983b (5)).

Two male and two female blind adults, who are accomplished readers of embossed braille, assisted in refining the Inkbraille code. (None of these subjects consistently use the Optacon in daily life, but all have recieved Optacon training.) The work of refining the Inkbraille code consisted of varying the dot size in the Inkbraille cells as well as the overall cell size and cell spacing, and the text line spacing, all in an attempt to discover the dimensions and proportions that would produce optimal machine-readability. Subjects were asked to read a number of the experimental versions of Inkbraille with the Optacon. Their comments, reactions, and performance, along with the authors' observations, were used as indicators of the potential readability of a particular version of Inkbraille.

Learning to use Inkbraille with the Optacon—Two of the subjects also participated in an investigation of the phenomenon of learning to read Inkbraille with the Optacon. One of these subjects read a total of 14 Inkbraille texts during 3 experimental sessions over a period of about 3 weeks. The second of these 2 subjects read a total of 24 Inkbraille texts; these texts were read during 6 experimental sessions covering a period of about 6 weeks. In addition, this subject also read nine letterprint texts with the Optacon[b], and six embossed braille texts, over the course of the six sessions. A tracking-aid[c] was used with the Optacon by both of these subjects, at their own request.

Immediately after silently reading each text, the subjects were asked for a verbal summary of the text. The Inkbraille reading performance data obtained from these two subjects (3 sessions employing 14 texts, and 6 sessions employing 24 texts) were used to explore the phenomenon of reading-skill acquisition, using Inkbraille. The reading data for embossed braille, and for letterprint read with the Optacon, have been used for comparative purposes and are believed to have facilitated a more reliable interpretation of the Inkbraille reading data.

During experimental reading, the instantaneous position of the subject's text-scanning hand(s) or the Optacon camera was monitored and recorded. This was accomplished through the use of a model C1373 Hammamatsu position-sensing system design-

[a]This work was supported by the Veterans Administration and the Biomedical Research Support Grant, University of Illinois at Chicago.

[b]The Optacon presents letterprint tactually by means of letter configurations on its field of vibrating pins.

[c]A tracking aid is a device that helps a blind reader move the hand-held sensing element or camera of a reading machine accurately along the lines of printed text, shift from line to line, etc.

ed to determine the simultaneous position of up to four infrared-light-emitting diodes. The horizontal and vertical position of the hand within the reading field was obtained by attaching an infrared diode to the Optacon camera for letterprint and Inkbraille reading, and to the index fingers of both hands for embossed-braille reading. The horizontal and vertical hand-position voltages from the Hammamatsu system, which were proportional to respective reading field position, were recorded on a multichannel chart recorder. This position information, along with the position information obtained from calibration marks, was used to determine the reading performance reported herein.

Most of the text materials were obtained from the Readers Digest column "Life in These United States." Both the letterprint and Inkbraille texts were prepared on single sheets of white paper with six calibration marks which were used to precisely locate the text in the reading field. The letterprint texts were produced using a Prestige Elite 96 type font having 12 letter-spaces per inch and 6 lines per inch. The text lines were about 70 letter-spaces in length.

The Inkbraille texts used during the refinement stage of this study varied in the size of the Inkbraille cell and the number of lines-per-inch of text field.

The embossed braille texts were produced manually with a Perkins Brailler and included calibration marks above and below the embossed text. The embossed braille texts, and the final version of the Inkbraille texts, both had about 40 cells per line, and were encoded in grade II braille.

The overall average length of the texts for all 3 modes of tactual reading was slightly less than 75 words.

Production of Inkbraille texts was accomplished through the use of an Apple II computer, a Diablo 1620 daisy-wheel printer, some accessories, and two software packages. A software package called Braille-Edit (Holladay, 1982 (6)) permitted the entry of text from the Apple II keyboard. This text information was translated into a grade II braille Apple text file by the Braille-Edit program. A second program (developed by Dr. Robert Stepp of the University of Ilinois at Urbana-Champaign) was then used to convert the grade II Apple text files into Inkbraille text via the Diablo printer.

The current version of Inkbraille was decided upon after some consideration of available dot sizes, the porportions of the standard embossed braille cell, and (most importantly) the apparent readability of the various versions with which we experimented. After some experimentation with several dot sizes we decided to use the period sign of the Diablo "Greek-math" printwheel for the dots of the Inkbraille cell. Further experimentation resulted in an Inkbraille code of 10 cells per inch of line, and 4 lines per inch of text. The current version of the Inkbraille cell is composed of dots 0.017 inches in diameter. The center-to-center horizontal distances between the columns of the cell are 0.033 inches; the vertical distance between rows of the cell is 0.042 inches between centers. The space between adjacent cells in a line is 0.067 inches from the center of the second column of one cell to the center of the first column of the second cell. The vertical distance between the center of the third row of a cell in one line to the center of the first row of a cell in the next line is 0.250 inches.

When read with the Optacon, this size of Inkbraille cell enabled the reader to adjust the size of the vibrating-pin tactual image over a range from smaller than the common embossed braille cell to larger than such a cell. It is anticipated that furthur refinements may result in even more reduction in the space required for a given amount of braille-encoded text, without undesirably limiting possible size of tactual image or otherwise increasing the difficulty of a reader's task.

Fig. 2 demonstrates the relative size of the language elements of the embossed braille, Inkbraille, and letterprint codes. When text is encoded in standard embossed braille, a page area of 10 square inches can contain up to a maximum of 100 braille cells. The same area may contain up to 298 Inkbraille cells (current version), or up to 719 letters and letter spaces (12 letter spaces/6 lines per inch). Based on these figures, Inkbraille reduces the spatial requirements for a given text by greater than 66 percent

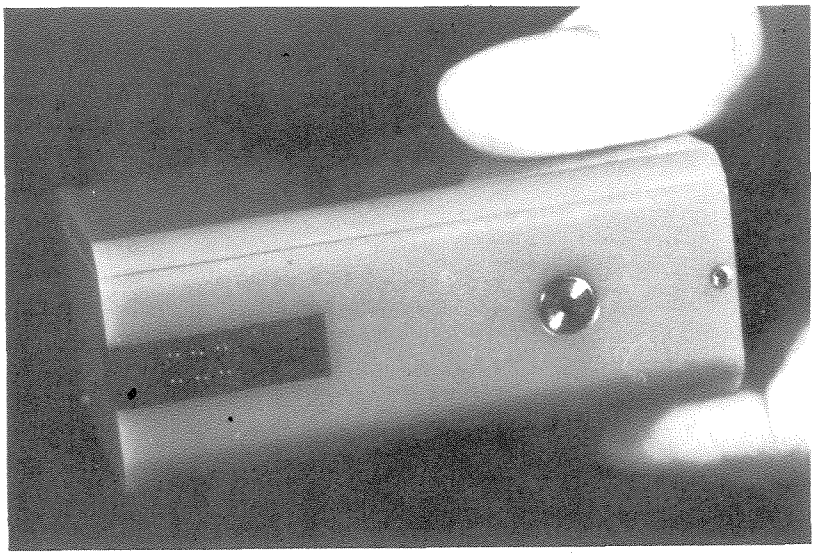

FIGURE 1
This is a conceptual model of a self-contained (except for a battery pack) handheld Inkbraille translator. The dimensions of this model (only 2½ inches long, and 1 inch by 1.6 inches in width and height) were determined by the authors using the actual space requirements of the necessary optical, photosensing, electronic, and tactile-stimulating components. The device represented by this model had not yet been built when the work described was done, and an Opticon was substituted. Note that the model's tactual output, two rows of three elements each, mimics the configuration of embossed braille. An Optacon has a multiple-pin field designed to present letter-print images.

when compared with embossed braille. By simply reducing the line spacing of Inkbraille to the equivalent embossed braille line spacing, the spatial requirements could be reduced by more than 80 percent.

Results

All four subjects were able to read the Optacon tactual output from Inkbraille upon initial exposure, and furthermore after limited exposure and practice there was significant improvement in reading performance.

The data for the subject who read 14 texts in three sessions show the Inkbraille reading rate nearly tripling from the first to the third session—She averaged 8.3 wpm for the first session (4 texts), 12.1 wpm for the second session (5 texts), and 22.0 wpm for the third session (5 texts). A gross measure of Optacon letterprint reading performance by the same subject was obtained by others at the time of this pilot study as a comparative measure: they reported a two-text average performance of 13.5 wpm by the subject for Optacon letterprint reading.

Inkbraille reading rate for the subject who read 24 texts in 6 session (4 texts per session) more than doubled from the first to the second session, thereafter remained about constant. Reading rates recorded for Inkbraille using the Optacon tactual output were 9.1 wpm (first session), 19.8 wpm (second session), 20.4 wpm (third session), 21.0 wpm (fourth session), 19.9 wpm (fifth session), and 18.3 wpm (sixth session).

As she did with her Inkbraille reading performance, the six-session subject demonstrated an improvement in her letterprint reading rate over the course of the six sessions. This result was anticipated, as this subject did not have routine access to an Optacon; she was Optacon-trained, but not practiced, and subsequent to training had only limited exposure to the Optacon. Her letterprint reading performance was 8.7 wpm (first session, one text), 11.9 wpm (second session, one text), 15.6 wpm (third session, one text), 13.8 wpm (fourth session, one text), 20.5 wpm (fifth session, one text), and 15.5 wpm (sixth session, 4 texts).

Embossed braille reading rate for this subject appeared to be relatively constant over the six sessions. This was to be expected of this skilled embossed braille reader, who attained an overall average (six texts, one for each of the six sessions) of 126 wpm.

After reading each text, both of these subjects (three-session and six-session) were asked, as mentioned previously, to summarize the material they had read. In virtually every instance, these subjects came close to a word-for-word recall of the text materials.

Discussion

It would appear from the data that only limited exposure to Inkbraille is needed in order to become familiar with this new mode of reading the tactual braille code. The obeservation that the three-session subject demonstrated a continual improvement across three sessions makes it difficult to speculate as to what rate she might eventually attain. However, in the case of the six-session subject, the fact that her performance seemed to be relatively constant after the second session tempts one to speculate that the learning phenomenon associated with the acquisition of Inkbraille reading skills might be a short-term process.

Embossed braille reading performance, which sets the current performance goal for any tactual-reading alternative, must be attributed to one or more of the distinctive features of the medium. One of these features is the standardized and rather simple punctate braille code. Since this feature is retained in Inkbraille, it was rather surprising that the use of Inkbraille did not result in higher reading rates. The embossed braille reading rate we observed in one subject was 126 wpm —that same subject attained a rate of 18.3 wpm for Inkbraille reading—during the sixth session! Thus, this subject read embossed braille (directly) almost seven times faster than Inkbraille (via the Optacon's tactual presentation). It is conceivable that a more optimal Inkbraille format, or additional practice and exposure, could improve Inkbraille reading rates. It seems doubtful, however, that either of these factors could lead to a sevenfold increase in rate. How does one explain the large differences between Inkbraille and embossed braille reading rates? One possible explanation is discussed in the following paragraphs.

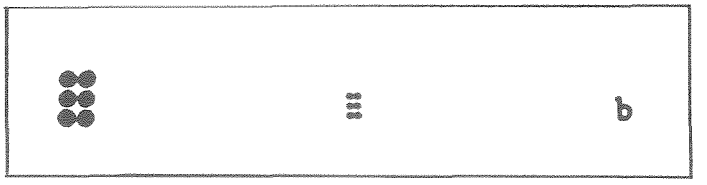

FIGURE 2
Relative size comparison of embossed braille (left), Inkbraille (center), and letter print.

The data for both subjects show their Inkbraille reading rates to be somewhat higher than their letterprint reading rates, using the Optacon in each case. The three-session subject attained a rate of 22 wpm with Inkbraille (third session) as compared to the 13.5 wpm we have for her letterprint reading performance. For the six-session subject the comparison is 18.3 wpm for Inkbraille versus 15.5 wpm for letterprint (sixth session). A given text will contain the same number of words, whether produced in braille or letterprint, but the braille version will contain fewer symbols than the print version, because of the contractions in braille. Since the braille version of the texts contains fewer symbols it will be read in a shorter time (Hislop, Zuber and Trimble, 1982 (4), 1983 (5). Thus, when reading rate is expressed in words per minute, it will appear that the braille is read faster than the print version. However, when these reading rates are adjusted for the effect of contractions in braille, the rates for Inkbraille and letterprint are virtually the same. Thus, we concluded that our subjects read Inkbraille and letterprint with the Optacon at the same rate.

This similarity of Inkbraille-cell and letter-symbol reading rates leads us to speculate that the Optacon (or some aspect of the Optacon reading process) could be the source of the rate-limiting constraints imposed on our subjects. It is obvious that the Optacon with its 144-pin vibrating array (6 columns × 24 rows), presents the reader with a tactile stimulus significantly different in nature from that of embossed braille. Additional limitations could arise from the fact that use of the Optacon requires two hands; one hand for manipulation (scanning) of the text and the other for tactual reception and interpretation of the vibrating-pin facsimile of the reading field. Regardless of the exact nature and extent of the limitations imposed on Inkbraille/Optacon readers, the tactile display of the Optacon, while appropriately designed with high resolution for letter-print translation, is not particularly well suited for the simple six-element display requirements of Inkbraille.

In summary, the authors conclude that Inkbraille can be easily read by the blind, and that significant increases in reading rate

can be accomplished after relatively little exposure. When Inkbraille is read with the Optacon as in the experiments reported here, reading rates are far below those for direct reading of embossed braille. Since there is little difference in reading rates for Inkbraille and letter-print when both are read with the Optacon, we conclude that the Optacon introduces a rate-limiting constraint. This is not entirely unexpected. The Optacon, appropiately designed with the high resolution required for the tactual reading of letter-print (but inappropriate for the simpler braille code), was used in this study primarily for purposes of expediency. We hope that higher reading rates can be achieved when Inkbraille is read with a device which is specifically designed to transform Inkbraille into a more apropriate pattern of raised elements. Our current efforts are directed toward the development of such a device ■

Acknowledgements

We thank Mr. Harvey Lauer and Mr. Leonard Mowinski of the Hines Veterans Administration Hospital Blind Center for their considerable help in producing the embossed braille and Inkbraille texts used in this study.

A note of thanks is also in order to Dr. Robert Stepp of the University of Illinois at Urbana-Champaign, who graciously provided part of the software used to produce Inkbraille.

REFERENCES

1. Foulke E: Reading braille. **In**: Tactual Perception: A Sourcebook. (Schiff W and Foulke E, eds) New York: Cambridge University Press, 1982.
2. Hislop DW, Zuber BL and Trimble JL: Skill-acquistion: the blind reading Inkbraille. Proceedings of 67th Annual Meeting of the Federation of American Societies for Experimental Biology, Chicago, Illinois, April 10-15, 1983.
3. Bliss JC, Katcher MH, Rogers CH and Shepard RP: Optical-to-tactile image conversion for the blind. IEEE Transactions on Man-Machine Systems, MMS-11(1):58-65,1970.
4. Hislop DW, Zuber BL and Trimble JL: Characteristics of blind reading and manual scanning with an electronic reading aid. Proceedings of the Fifth Annual Conference on Rehabilitation Engineering, Bethesda, Maryland, Rehabilitation Society of North America, 1982.
5. Hislop DW, Zuber BL and Trimble JL: Characteristics of reading rate and manual scanning patterns of blind Optacon readers. Human Factors 25(4):379-389,1983.
6. Holladay D: Computer applications to braille. J Vis Impair and Blind 324-325, Oct 1982.

Compressive Behavior after Simulated Service Conditions of Some Foamed Materials Intended as Orthotic Shoe Insoles

G. J. CAMPBELL, Ph.D., P.Eng., C.C.E.[a]
Department of Biomedical Engineering
University Hospital
London, Ontario, Canada

M. McLURE, B.Sc.(OT)
E. N. NEWELL, M.D., F.R.C.P.(C)
Department of Physical Medicine and Rehabilitation
University of Western Ontario
London, Ontario, Canada

Abstract—The compressive characteristics of a group of foamed plastics and rubbers, suitable for use as orthotic shoe insoles, were assessed for any changes incurred as a result of exposure to a series of simulated service conditions. The service conditions considered in this study were heat (accelerated aging), sustained deflection (compression set), and cyclic loading. Since the stress/strain characteristics computed from the load/deformation curves were non-linear, it was necessary to develop a new procedure for comparing the relative compressive characteristics. The results from this study identified a group of preferred materials whose virgin compressive characteristics have been judged to be the most suitable, and which exhibited the least change following exposure to the three simulated service conditions.

Introduction

An increasing number of foamed plastics and rubbers have shown promise in the field of prosthetics and orthotics because of the ease and speed with which they can be used. Shoe insoles of the "accommodating" type, fabricated from such materials, are regarded as having "cushioning" (Orders, 1977 (1); Albert, 1982 (2)) or "pressure-distributing" (Mann, 1978 (3); Wood, 1981 (4)) properties, and are generally felt to function as soft-tissue supplements*.

The objective and clinical data to support these contentions is presently lacking. The functional anatomy and biomechanics of the foot,and the mechanical characteristics of the soft tissues, are not completely understood (Stokes et al, 1979 (5), Ziegert and Lewis, 1978 (6)). It has been acknowledged, however, that matching the mechanical characteristics of the tissues of the foot with those of the material would be useful (Beach and Thompson, 1979 (7)).

Our research group has initiated a project to determine the mechanical characteristics of a group of orthotic materials (see Appendix A for a complete list) and to provide comparisons among these same materials. Previous compression testing of the materials (Campbell et al, 1982 (8)) indicated that the materials could be divided into three distinct categories, (i) very stiff, (ii)

[a]Please address all correspondence to: Dr. G J. Campbell, Department of Biomedical Engineering, University Hospital, P.O. Box 5339, Terminal A, London, Ontario, Canada, N6A 5A5

*Personal communication, R. Rhodes, 1979.

moderately deformable, and (iii) highly deformable, with the majority of the materials in the moderately deformable category.

The environment of the shoe-foot component, and the stresses to which the foot is exposed during rest and activity, were reviewed. The effects of heat, perspiration, and sustained and repetitive compressive loading as well as shear loading, were all considered by us to influence the effectiveness of orthotic shoe insoles. Ideally, the stimulation of the shoe-foot environment should include all of the factors cited above. The assessment of shear loading alone, of perspiration, and of combined compressive and shear loading would require the development of original test procedures. We decided instead to assess the influence of heat, of sustained loading, and of repetitive loading by adapting existing standard test procedures. This obviously partial series of simulation procedures represents an initial investigation to determine which factors influence the compressive characteristics of a group of orthotic materials. It is hoped that suitable test procedures to assess the remaining factors will be developed in the future.

Materials and Methods

The various test procedures for foamed plastic and rubbers published by the American Society for Testing and Materials (ASTM) were reviewed. Test procedures were selected that closely approximated the service conditions to be investigated. In the case of heat, the ASTM test procedure for accelerated aging was selected. Sustained loading was assessed by the ASTM test procedure for compression set, while the assessment of repeated loading made use of a device specifically designed to provide the desired loading condition.

Heat—The test procedure to assess this service condition is a modification of ASTM Designation D573-67 titled "Standard Method of Test for Accelerated Aging of Vulcanized Rubber by the Oven Method" (9). Square specimens measuring about 500 mm along each side were cut from each of the 31 materials. The thickness was measured using a modified dial micrometer with a large foot and constant-contact load.

The specimens were then suspended vertically in an air-circulating oven, arranged so that no specimen impinged upon another or upon the walls of the oven. The specimens remained in the oven for a period of 7 days at a temperature of 41 deg C. Oven temperature was established using a thermistor inserted between the foot and shoe of two volunteers, remaining in place for an hour. This provided a measure of the temperature which resulted from the heat accumulation.

Following the period of 7 days the materials were removed and permitted to cool in the horizontal position for 24 hours. Standard circular specimens (2.85 cm diameter) were cut from each of the materials and the thickness was again measured. Each specimen was then placed on the lower platen of a Materials Testing Machine (Instron Model 1125) and loaded in compression at rates of 10 mm/min and 100 mm/min to a maximum of 23 kg (stress of 3.6 kg/cm² or 353 MPa). This stress is slightly in excess of the maximum stress for the foot during walking calculated by Godfrey et al, 1967 (10).

Sustained Loading—The test procedure used to assess this service condition was ASTM D395 "Standard Methods of Test For Compression Set of Vulcanized Rubber" (11). This procedure requires that specimens be compressed at a known deformation, between two parallel plates. The apparatus assembled for this purpose is illustrated in Figure 1. Standard circular specimens (2.85 cm diameter) were cut from the material and the thickness of each was measured with the modified dial micrometer. The test procedures differed slightly depending upon the cellular construction of the material (Plies of each open-cell foam were stacked to a minimum height of 6 mm, but only one ply of the closed-cell foams was used.) Specimens were then placed in the cylindrical cavity of the test jig and the plunger inserted. The material was compressed by a clamp until the specimen was reduced to 50 percent of the original thickness (Fig. 1). The material was maintained in compression at room temperature for a period of 7 days. The clamp was then released and the specimen removed from the jig. The thickness of the specimen was measured immediately following removal, as well as after a delay of 30 minutes. The specimen was then placed on the lower platen of the testing machine and the compression test described in the previous test procedure was repeated.

Repetitive Loading—The procedure for determining the effects of repetitive loading was developed by our group. Standard circular specimens (2.85 cm diameter) were cut from the materials and the thickness of each measured with the modified dial micrometer. Each specimen was then mounted on the base of a cyclic loading apparatus which had been designed and fabricated for the purpose of this study (Fig. 2). The specimen was loaded in compression to a maximum of 3 kg/cm² or 294 MPa at a rate of about 1 Hz. Each specimen was subjected to a minimum of 250,000 cycles which represents the approximate number of steps for a 3-month period*. The specimens were removed from the apparatus and the thickness measured immediately with the modified dial micrometer. The specimen was placed on the lower platen of the testing machine and the compression test described previously was repeated. A second thickness measurement was performed 30 minutes after removal of the specimen from the cyclic loading apparatus.

The load deformation records obtained with the testing machine were converted into stress/strain curves. The stress (σ) is computed as "engineering stress" which is defined by the relationship:

$$\sigma = \frac{P}{A}$$

where P = the applied load and A = the cross-sectional area (constant).

The strain (ϵ) or deformation is calculated by the equation:

$$\epsilon = \frac{\Delta L}{L}$$

where ΔL = the change in thickness and L = the original thickness.

The materials under consideration in this investigation exhibited a non-linear stress/strain relationship. Since the principal objective of this study was to compare the compression properties of the materials following the simulated service conditions with the original compression characteristics of the materials, the

*Personal communication, J. Holden, 1979.

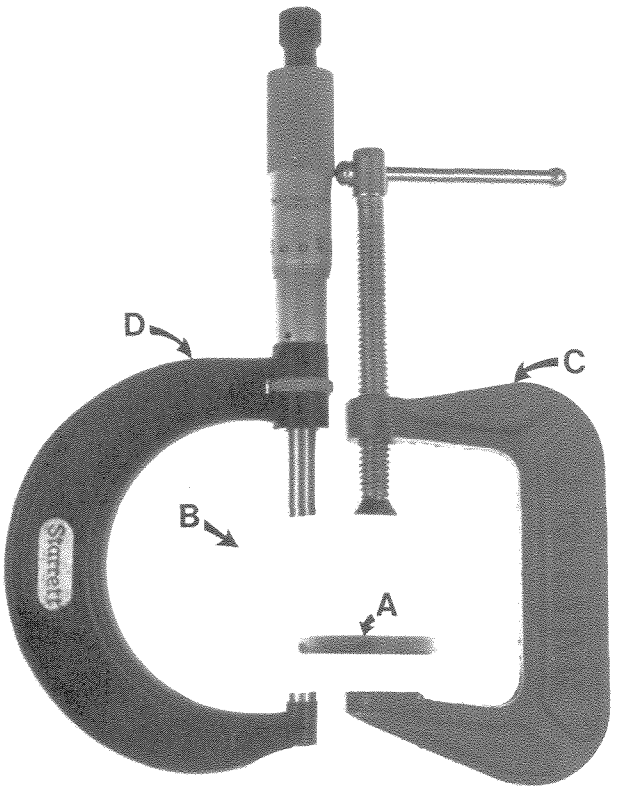

FIGURE 1
The jig for maintaining the compression of a material.
A-Specimen within test jig
B-Test jig
C-Clamp
D-Micrometer

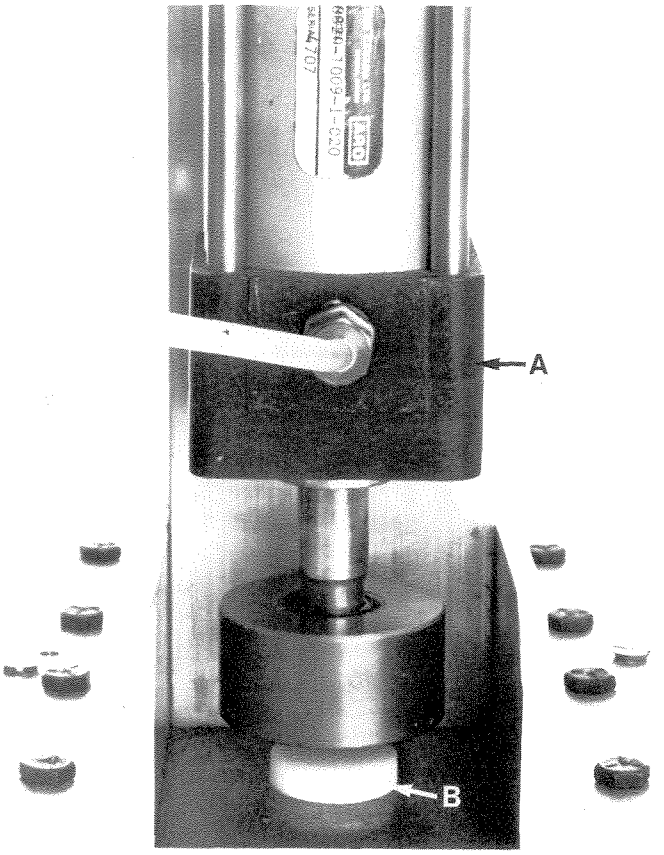

FIGURE 2
Cyclic loading apparatus.
A-Pneumatic cylinder
B-Specimen

standard techniques such as the comparison of slopes or strain energy (area beneath the stress/strain curve) were not judged appropriate. A new method has been devised that first divides the range of stress (0 to 3.0 kg/cm² or 0 to 294 MPa) into a series of equal increments (0.2 kg/cm² or 19.6 MPa). At each stress increment, the ratio of the strain for the material that had been subjected to the service condition, divided by the strain for the virgin material, was computed. This proportion was then converted to the equivalent log of the proportion to the base 10. The term "Log Standardized Strain" (LSS) has been chosen to identify this calculation.

A typical stress/strain plot of the virgin material is depicted as curve A in Figure 3. The hypothetical stress/strain plots for samples of the same material after being subjected to two different service conditions are depicted in the same figure by curves B and C.

The plots for the LSS vs the stress increments for curves B and C are shown in Figure 4. The zero axis represents the compressive properties of the virgin material. A positive value for the LSS indicates an increase in the strain at the same stress, while a negative value indicates a decrease in the strain at the same stress level. Curve B in the stress/strain plot demonstrated a sustained shift to greater strain which is reflected by the positive offset in the LSS plot (Fig. 4). Curve C on the stress/strain plot demonstrated an initial decrease in the strain relative to the virgin material, until it crossed over the plot for the virgin material. The relative change in the initial portion of curve C is reflected by the negative values in Figure 4, followed by the crossover and positive values for the final portion of the curve.

The relationship between the magnitudes of curves B and C is also affected by a log relationship. For example, at the stress of 2 kg/cm² in Figure 3, the strain for the virgin material (curve A) was 52 percent. For curve B, this strain (at the same stress) had increased to 66.5 percent, which represents a proportional increase of 1.28 with respect to the virgin material. However, the magnitude on the LSS plot equivalent to the proportional increase at 2 kg/cm² is 0.195. The benefit of converting the proportional strains to Log Standardized Strains is that the relative differences (both <1 and >1) are spatially equivalent. For example, the spatial difference for a proportional increase of two is the same as the spatial difference for a proportional decrease of one half with respect to the original curve for the virgin material. We feel that this method facilitates the visual interpretation of nonlinear relationships. If the log had not been computed, then changes in the material that resulted in greater values of strain (e.g. two times) would appear to be disproportionally larger than the inverse relative change (e.g., one-half times) for decreased values of strain.

During the ensuing explanation, the results for the compressive characteristics (stress/strain) of the virgin material would be

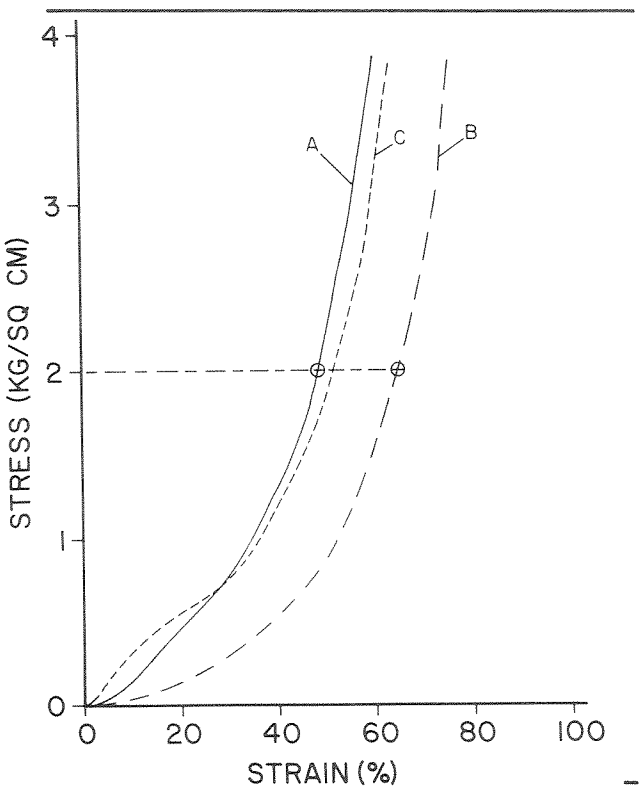

FIGURE 3
Hypothetical stress-strain curves representing the compression characteristics of the virgin material (A), after service condition (B) and after service condition (C).

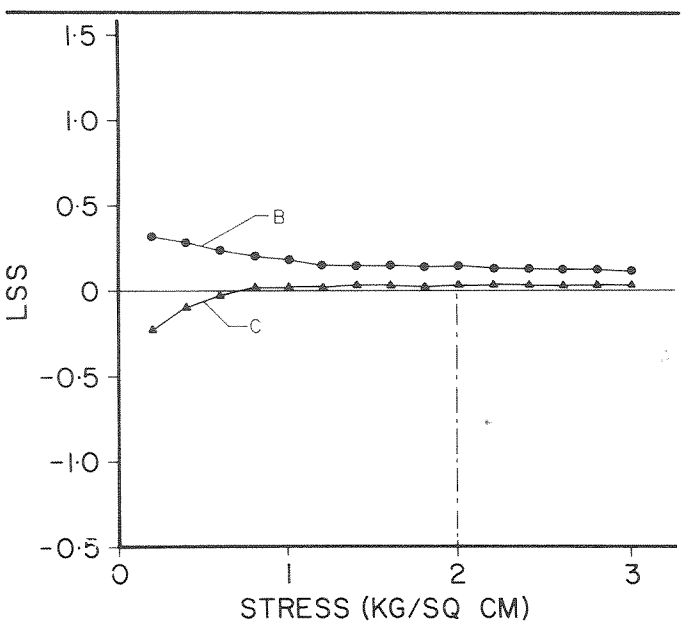

FIGURE 4
Graph of Log Standardized Strain (LSS) and stress for each of the two service conditions (B and C) presented in Figure 3.

similar to curve A. The compressive characteristics (stress/strain) of the same material following exposure to the various service conditions would be represented by curves B and C. Curves B and C will be presented as the Log Standardized Strain.

Results

Compressive Tests—In the interest of brevity, only the LSS for materials representative of a group, or the LSS of a material demonstrating either interesting or unusual deviations, will be presented graphically.

An examination of the data for the 31 materials investigated in this study revealed a number of materials with characteristics that did not deviate substantially (i.e., <0.2 Log Standardized Strain) from the virgin material. A representative result for this group is presented in Figure 5. These materials have been identified as Group 1:

GROUP 1

Ensolite* (3.2 mm thick)
Evazote* (12.7 mm thick)
Aliplast 4E*
Poron 'Sport'
Polyurethane
Dr, Scholl's Cushion Insole
Odor-Eaters
Carpet Wool (pile weight of 1.15 kg/cm²)
Carpet Polypropylene (pile weight of 0.74 kg/cm²)

Only the cyclic loading characteristics for the materials marked with an asterisk (*) show significant deviation (>0.1 but <0.2 Log Standardized Strain) for the service conditions of sustained loading and heat.

The characteristics for a second group of materials also did not generally demonstrate a deviation (i.e., <0.2 Log Standardized Strain) from the virgin material—except in the initial portion of the curve. Figure 6 illustrates the results for neoprene R 425 N (3.2 mm thick) which is representative of the results for the remaining materials in this group. In each case the positive results for the initial portion of the curves indicate that the material exhibited a greater strain, similar to the hypothetical curve B in Figure 4. The materials in Group 2 are:

GROUP 2

Celtite
neoprene R 425 N (3.2 mm, 6.34 mm thick)
neoprene R 431 N (3.2 mm thick)
Lynco
Ensolite (6.35 mm thick)
Evazote (1.6 mm thick)
Spenco

The only material with a negative initial portion of the LSS curve was Spenco (accelerated aging).

A third group,which demonstrated similar changes greater than 0.2 Log Standardized Strain for two materials, is illustrated by Figure 7. The two materials in Group 3 are:

GROUP 3

neoprene R 431 N (3.2 mm thick)
Bonfoam

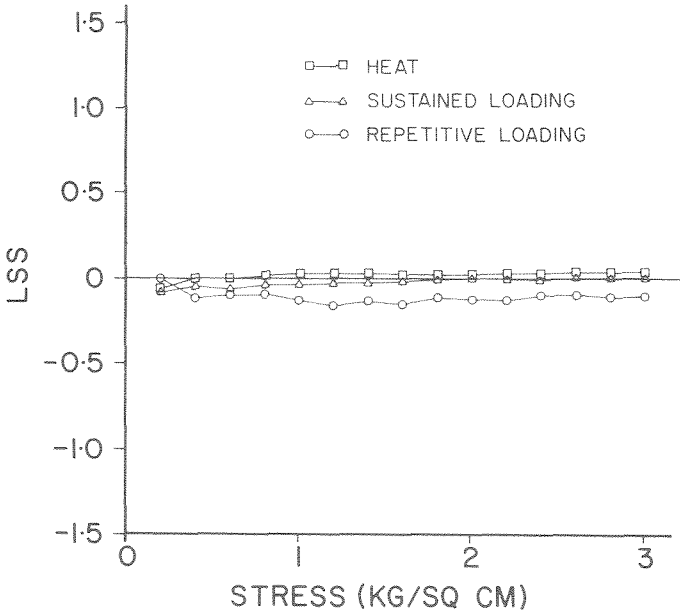

FIGURE 5
The LSS versus stress plot for Ensolite (3.2 mm thick).

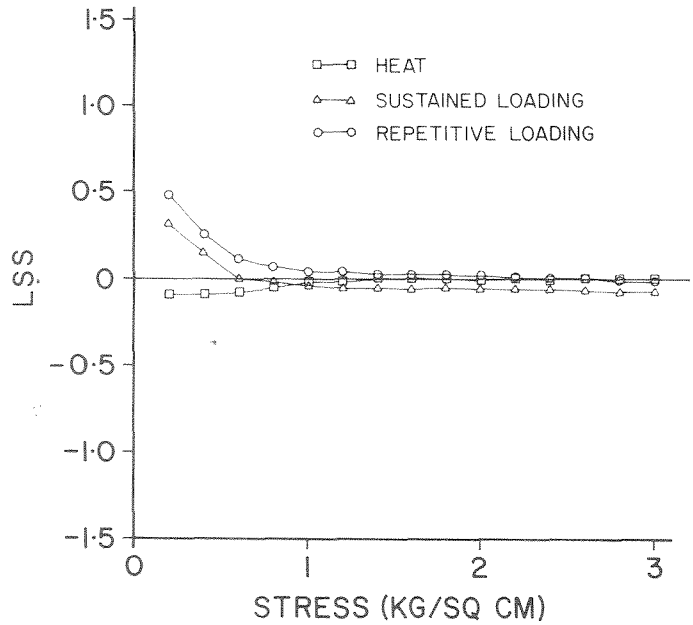

FIGURE 6
The LSS versus stress plot for Neoprene R 425 N (3.2 mm thick)

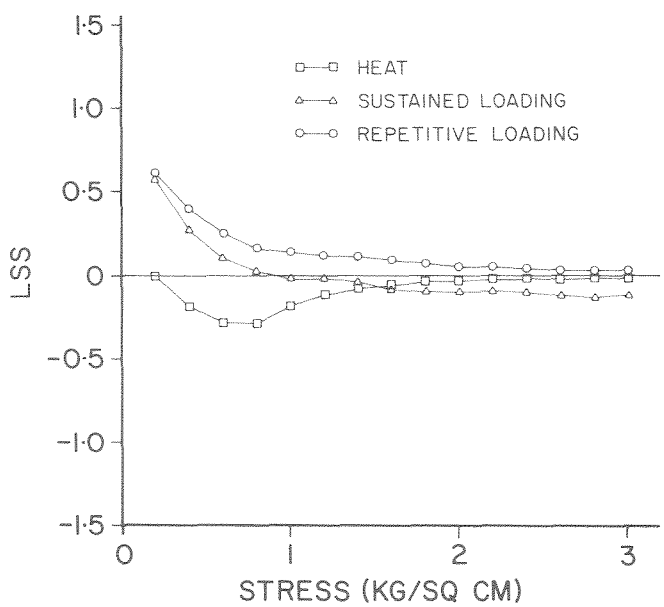

FIGURE 7
The LSS versus stress plot for Neoprene R 431 N (3.2 mm thick)

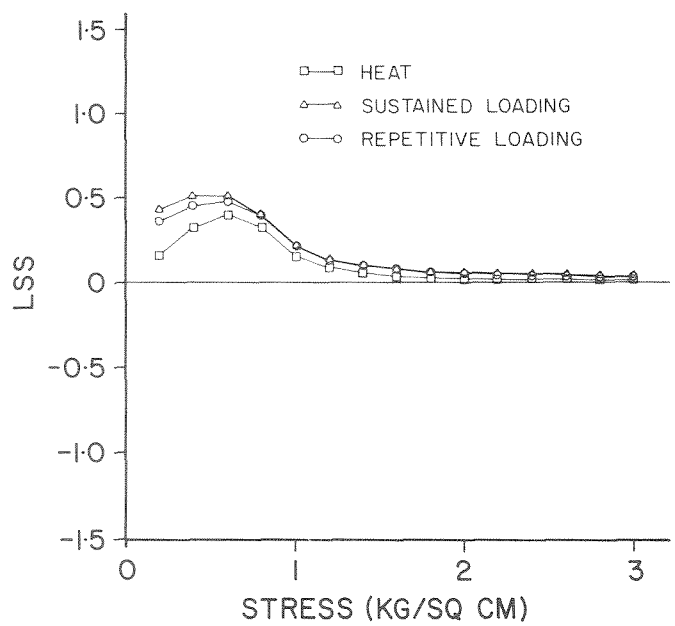

FIGURE 8
The LSS versus stress plot for Poron 20125

The remaining materials could not be readily grouped according to any consistent pattern or trend. Nevertheless, a series of materials demonstrated only moderate changes. In the case of Ethafoam, the accelerated aging and compression set were virtually unchanged, but the results for the cyclic loading were similar to the results (cyclic loading) for Group III materials. The results for compression set associated with high density Neoprene also showed a major sustained deviation, whereas the other test results were not distinctly different from the virgin material. In the case of Poron 20125, the results (Fig. 8) showed a similar deviation (described as a hump associated with the initial portion of the curve). The results for Poron 17125 also demonstrated a consistent deviation that was the mirror image to Poron 20125 but on the opposite side of the LSS axis. The results for Pelite (12.7 mm thick) were similar to the Group I materials, but demonstrated a distinct positive offset. Results for Pacer demonstrated a distinct offset (both positive and negative) with the initial portion of the curve, but the offset was not evident for the final portion. Results for Plastazote (3.2 mm, 6.35 mm thick) were erratic for the initial portion of the curve but only the results for cyclic loading continued to exhibit a deviation for the final portion of the curve.

The results for the final group of materials can only be described as highly erratic as evidenced by the results presented in Figure 9. The materials in this group were:

GROUP 4

Kemblo
Pelite (1.6 mm thick)
Aliplast 6A
Aliplast 10

Thickness—The results for the thickness measurement, before and after heating, did not demonstrate a distinct change for any of the materials.

Many of the materials demonstrated diminished thickness following both sustained loading (Fig. 10) and repetitive loading (Fig. 11). The relative loss in thickness for each material was not always consistent for both types of loading. In most cases the material exhibited a greater thickness loss for repetitive loading than for sustained loading. Furthermore, there was considerable variability among the materials in their loss of thickness for repetitive loading while the losses were more uniform from material to material for the sustained loading.

The loss in thickness 30 minutes after release of the load did not deviate more than 10 percent from the results at 10 minutes following release of the load.

Discussion

During the selection process for an appropriate material applicable as an orthotic shoe insole, the compression characteristics are an important consideration. The ideal material should distribute the load to areas adjacent to the bony prominences. This material should be neither too hard (insufficient deformation) nor too soft so that the limit of deformation is reached, resulting in "bottoming out". The previous publication by our group (Campbell et al, 1982 (8)) has presented information on the compressive characteristics of the virgin material with the preferred material being one described as "moderately deformable".

A further consideration is the "durability" of the material; its ability to withstand these service conditions over time. In the case of orthotic shoe insoles, a material's resistance to heat, sustained compression, and repeated compression are considered to be important indicators of durability in the intended service.

The present study has identified a group of materials (groups 1 and 2) that did not change substantially in their compressive characteristics following exposure to the simulated service conditions. The materials whose compressive characteristics were identified by the previous study as preferred (moderately deformable) and also classified in the present study as the least affected by the simulated service conditions (i.e., groups 1 and 2) were:

Ensolite (3.2 mm thick)
Aliplast 4E
Carpet - Wool (pile weight of 1.15 kg/m²)
Celtite
neoprene R 431 N (6.34 mm thick)
Spenco
Evazote (12.7 mm thick)
Poron-'Sport'
Carpet - Polypropylene (pile weight of 0.74 kg/m²)
neoprene R 425 N (3.2 mm, 6.34 mm thick)
Lynco

It would be anticipated that a loss in thickness would diminish the "pressure-distributing" capabilities of a material, since less depth of material would be available to accomodate the contours of the foot. The materials identified in the previous study as preferred (moderately deformable) and also exhibiting less than 20 percent loss of thickness following **sustained** loading were:

Poron-20125
Poron-17125
Poron-'Sport'
Lynco

A similar comparison between the moderately deformable and less than 20 percent loss of thickness following **repetitive** loading identified the materials:

Poron-20125
Poron-17125
Poron-'Sport'
neoprene - R 431 N (3.2 mm thick)
neoprene - R 425 N (3.2 mm thick)
Bonfoam
Lynco

The only materials common to the preceding three selection procedures are:

Poron-'Sport' and Lynco

It is evident from the analysis of the data that an association does not necessarily exist between a small reduction in the

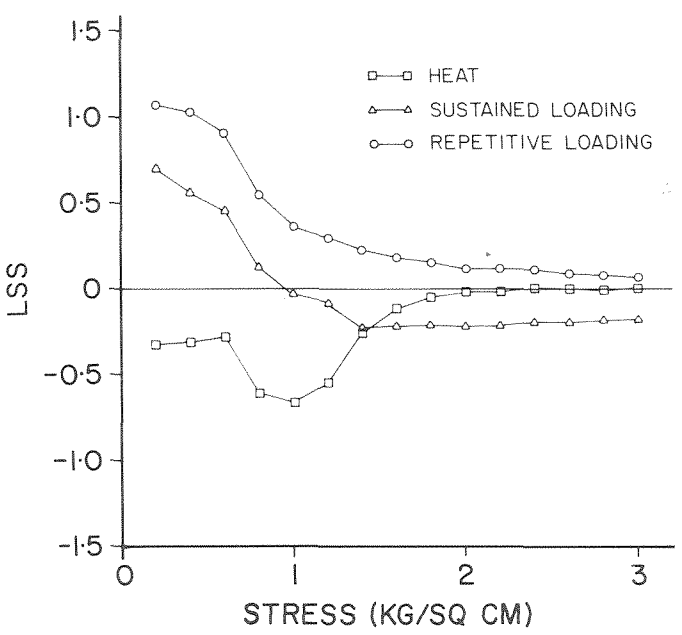

FIGURE 9
The LSS versus stress plot for Aliplast 6A.

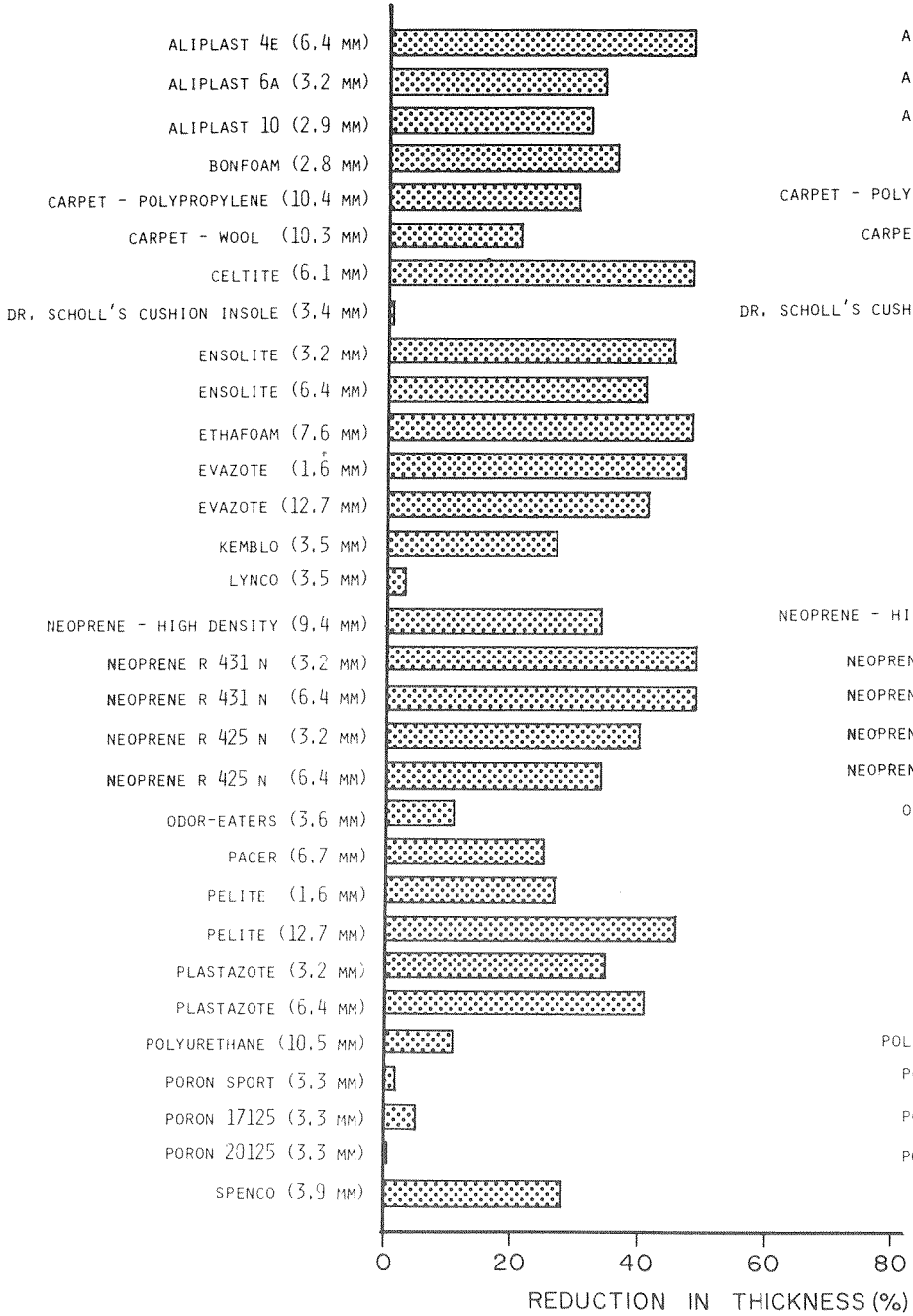

FIGURE 10
The loss in thickness following sustained loading (measurements in brackets indicate original thickness).

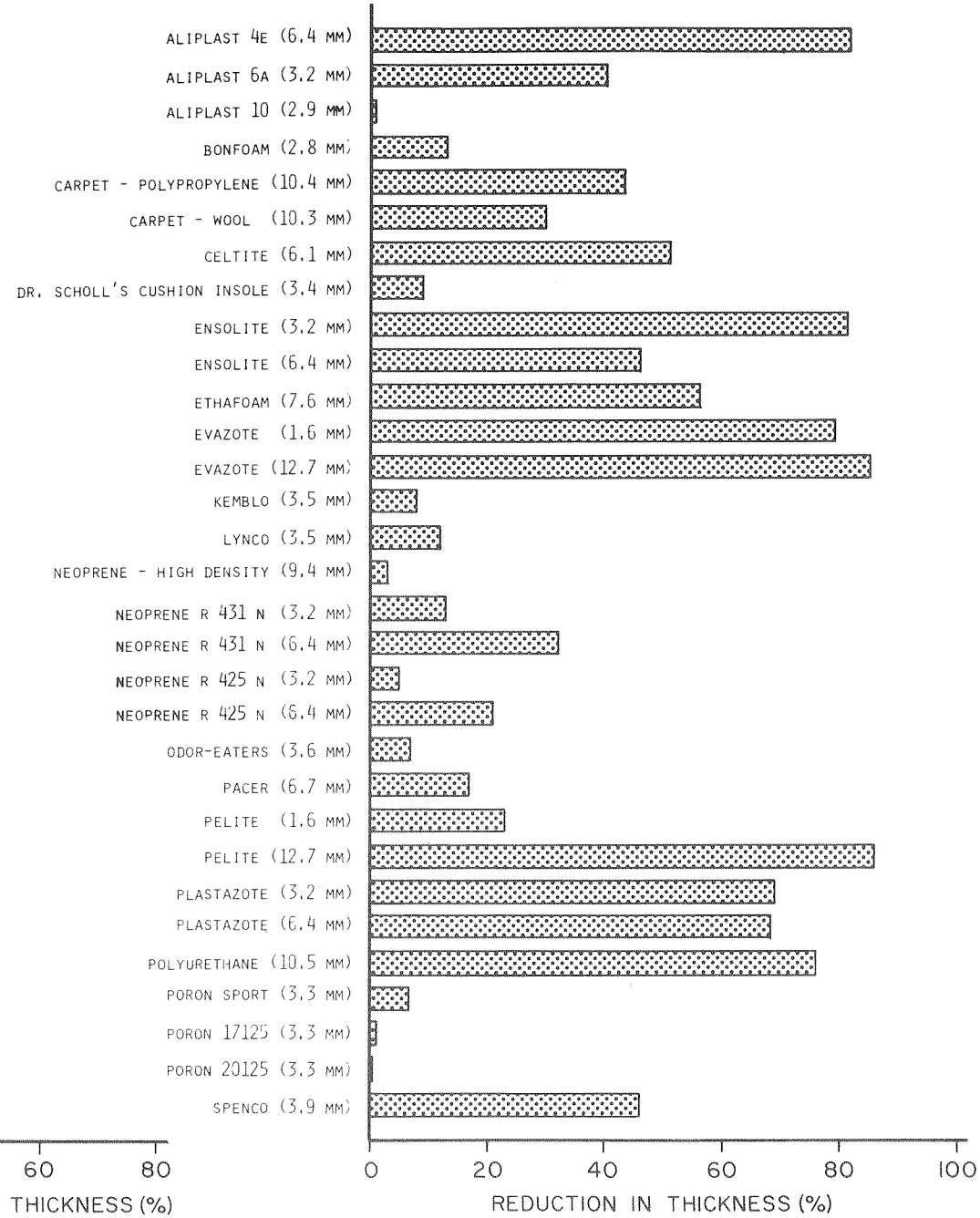

FIGURE 11
The loss in thickness following repetitive loading (measurements in brackets indicate original thickness).

thickness and the preferred compression characteristics.

The test procedures developed for this study measured the three service conditions separately, rather than in combination as would be the case during the use of any material as an orthotic shoe insert. The results for all the materials were examined to determine if a particular service condition exhibited a more severe influence on the compression characteristics. In most cases, where the results for the compression characteristics changed, repetitive loading had the most effect—in some cases, repetitive loading was the only service condition that resulted in a change.

It cannot be determined from the present study whether the assessment of the change in thickness or the change in LSS is to be preferred, since both are indicators of different characteristics. A comparative clinical evaluation, which assesses the compression characteristics and thickness with respect to effectiveness after a period of use by a group of subjects, would likely provide relevant results. However, the problem of monitoring the activity levels of the subjects complicates the interpretation of the results. The distinct advantage of our technique is that all materials have been subjected to identical service conditions.

There are other service conditions such as wear (fretting), rotary and translational shear, and perspiration that could also be considered. It is our hope to assess these additional characteristics in future investigations, as well as the clinical evaluation of representative materials from different groups ■

APPENDIX A

Source of foamed plastics and rubbers

Product designation*	Source**
Aliplast 4E, 6A, 10	Alimed 68 Harrison Avenue Boston, MA 02111 U.S.A. (671) 451-2240
Bonfoam	Georgia Bonded Fibres Inc. Buena Vista, VA 24416 U.S.A. (703) 261-2181
Celtite, Pelite, Lynco Evazote,Plastazote	Apex Foot Products Corp. 200 Forest Avenue Englewood, NJ 07631 U.S.A. (800) 526-4754 (201) 871-0807
Plastazote, Pelite	Orto Ped Inc. 6660 rue Clark Montreal, Quebec, Canada H2S 3E7 (514) 279-5266
Pacer	Carrier Shoe Co. 90 Ontario Street Toronto, Ontario, Canada M5A 3V6 (416) 363-5643
Poron	Rogers Corp. East Woodstock, CT 06244 U.S.A. (203) 928-7931
P.P.T. (Poron)	Langer Biomechanical Group 21 East Industry Court Deer Park, NY 11729 U.S.A. (800) 645-5520 (516) 667-3462
neoprene	Rubatex Corp. Bedford, VA 24523 U.S.A. (703) 586-2611
Ensolite, neoprene	Uniroyal Inc. Expanded Products Dept. Mishawaka, IN 46544 U.S.A. (219) 255-2181 Uniroyal Ltd. 51 Breithaupt Street Kitchener, Ontario, Canada N2H 5G5 (519) 744-4171
Ethafoam	Dow Chemical U.S.A. Functional Products and Systems Dept. Midland, MI 48640 U.S.A. Dow Chemical of Canada, Ltd. Modeland Road P.O. Box 1012 Sarnia, Ontario, Canada N7T 7K7 (519) 339-3641
Plastazote, Evazote	BXL Plastics Ltd. ERP Division 675 Mitcham Road Croydon, UK CR9 SAL 01-684-3622
Plastazote	Smith and Nephew Ltd. 2100-52nd Avenue Lachine 620, Quebec, Canada H8T 2Y5 (514) 636-0772

*Product designations with the exception of neoprene are believed to be registered trade names and have been treated as such except that the "registered" symbol usually shown for such names in this publication have been omitted to avoid distracting typographical clutter.

**Sources are those listed by the authors and are believed in most if not all cases to be manufacturers or leading authorized distributors.

REFERENCES

1. Orders C: A comparison in medium and low density plastazote in the fabrication of insoles. Can J Occ Ther 45(1):17-18,1977.
2. Albert S: A subjective comparison of Spenco and P.P.T. soft tissue supplements used in footgear. Ortho & Prosth 35(3):17-21, 1981.
3. Mann RA; Conservative Treatment and Office Procedures. **In** DuVries' Surgery of the Foot, 4th edition. The C.V. Mosby Company, Saint Louis, 1978.
4. Wood B: The Painful Foot. **In** A Textbook of Rheumatology (Kelley W, Harris E, Ruddy S, Sledge C, eds). W.B. Saunders Company, Philadelphia, pp 472-484, 1981.
5. Stokes IAF, Hutton WC, Stott JRR: Forces acting on the metatarsals during normal walking. J Anat 129(3):579-590, 1979.
6. Ziegert JC and Lewis JL: In vivo mechanical properties of soft tissue covering bony prominences. Trans ASME, J Biomech Eng 100:194-200, 1978.
7. Beach RB and Thompson DE: Selected soft-tissue research. An overview from Carville. Phys Ther 59(1):30-33, 1979.
8. Campbell G, Newell E, McLure M: Compression testing of foamed plastics and rubbers for use as orthotic shoe insoles. Prosth Ortho Int 6:48-52, 1982.
9. Standard Method of Test for Accelerated Aging of Vulcanized Rubber by the Oven Method. ASTM Designation: D 573-67. American National Standards Institute, pp 305-307, 1971.
10. Godfrey CM, Lawson GA, Stewart WA: A method for determination of pedal pressure changes during weight bearing: preliminary observations in normal and arthritic feet. Arthritis Rheum 10(2):135-140, 1967.
11. Standard Methods of Test for Compression Set of Vulcanized Rubber. ASTM Designation: D 395-68. American National Standards Institute, pp 195-201, 1971.

XX Standard Methods of Testing Slab Flexible Urethane Foam. ASTM Designation D 1564-71. American Society for Testing and Materials and The Society of the Plastics Industry, pp 719-736.

XX Standard Test Method for Flexural Fatigue of Plastics by Constant-Amplitude-of-Force. ANSI/ASTM D 671-71. American National Standards Institute, pp 253-261, 1978.